ENGINEERING RESEARCH JOURNAL (ERJ)
Vol. 1, No. 42 October 2019, pp.116-122.
Journal Homepage: www.feng.bu.edu.eg

Dynamic Response of Blast-Loaded RC Columns

Fouad B. A. Beshara, Youssef M. H. Hammad, and Mahmoud K. Ameen

Civil Engineering Department, Faculty of Engineering (Shoubra), Banha University

ABSTRACT:
This research paper presents a numerical procedure for predicting the nonlinear dynamic response of blast-loaded RC columns. A three-dimensional solid element and link element is used for spatial discretization of concrete and steel reinforcement, respectively. A summary of a rate- and history-dependent constitutive model is proposed for the progressive failure analysis of concrete under blast. The proposed model is an improved version of Riedel-Hiermaier-Thoma (RHT) model and accounts for different materials nonlinearities and strain rate sensitivity in compression and tension. The steel is modeled as a rate-dependent elasto-plastic material with strain hardening. The proposed model was implemented in the computer program AUTODYN. An explicit time integration scheme is followed for the nonlinear dynamic analysis. The proposed procedure was successfully used for predicting the dynamic response (failure modes, deflection-time histories, and acceleration-time curves) of several blast-loaded RC columns, tested before in the literatures.

Keywords: Blast loading; Reinforced concrete columns; Finite element modelling; Dynamic nonlinear analysis; RHT Concrete model; AUTODYN

1. Introduction

The ability of reinforced concrete to absorb energy under severe dynamic loading conditions has led to its utilization for structures, which may be subjected to impact or blast loadings. The low probability of occurrence of these loads necessitates design of such structures according to collapse limit state concept in which irreversible structural deformations and material damage are acceptable, provided that overall structural integrity is maintained [1-3]. For blast-loaded RC members, major sources of material nonlinearities such as progressive cracking of concrete in tension zones, inelastic response of concrete in compression, and inelastic deformation of reinforcing steel should be taken into consideration [4-7] during the dynamic analysis.

In this paper, a nonlinear constitutive law is suggested for nonlinear analysis of blast-loaded RC columns [8]. The material constitutive relations account for different nonlinearities for concrete and steel in compression and tension. Also, it considers the effect of stirrups-induced passive confinement in compression, and strain rate effects. The proposed law was implemented in the nonlinear dynamic analysis program, AUTODYN [9]. The enhanced hydrocode software has been successfully used for predicting the dynamic response of several square and rectangular blast-loaded RC columns, tested before in the literatures [10,11] in either displacement-time history or acceleration-time history curves.

2. Geometric Idealization of RC Columns

To represent concrete geometry in RC columns, the solid element (Solid 65) is used in AUTODYN program [9]. The element has eight nodes with three degrees of freedom at every node – translations within the nodal x, y, and z directions. The element is capable of plastic deformation, cracking in three perpendicular directions, and crushing. The geometry and node locations for this element sort are shown in Figure (1).

To discretize steel reinforcement in RC columns in AUTODYN program [9], 3-D spar element (Link 8) is utilized. The geometry and node locations for this element sort are shown in Figure (1). The element is capable of yielding and plastic deformation. For longitudinal steel bars, the element resists axial and flexural actions as required in RC columns under lateral blast loading. Simplified axial bar link elements are used for transverse stirrups in columns.

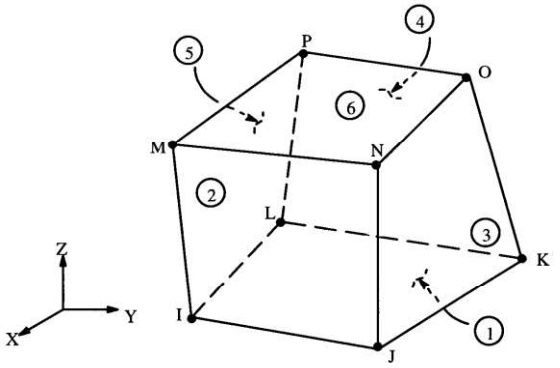

a) Solid 65 – 3D Reinforced Concrete Solid

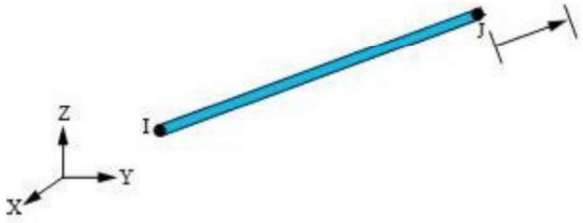

b) b) Link 8 – 3D spar

Fig. 1: Spatial Representation of Reinforced Concrete [9].

3. Material Modelling of Concrete

3.1 Failure Criteria for Concrete

The RHT (Riedel-Hiermaier-Thoma) model [8,9] shown in Figure (2) consists of three ultimate surfaces defined in failure surface, elastic limit surface and residual strength surface, describing the failure strength, initial yield strength and residual strength of the concrete respectively. The model can reflect the dynamic mechanical behavior of concrete material more completely because of that RHT model has become the worthiest of consideration for cement-based material. The profile of the failure surface and 3-D failure surface in principal stress space for the RHT concrete model is shown in Figure (2) which developed by taking into consideration the effect of confinement resulted from stirrups existence and the strain rate effect for reinforced concrete under blast loads in compression and tension [8].

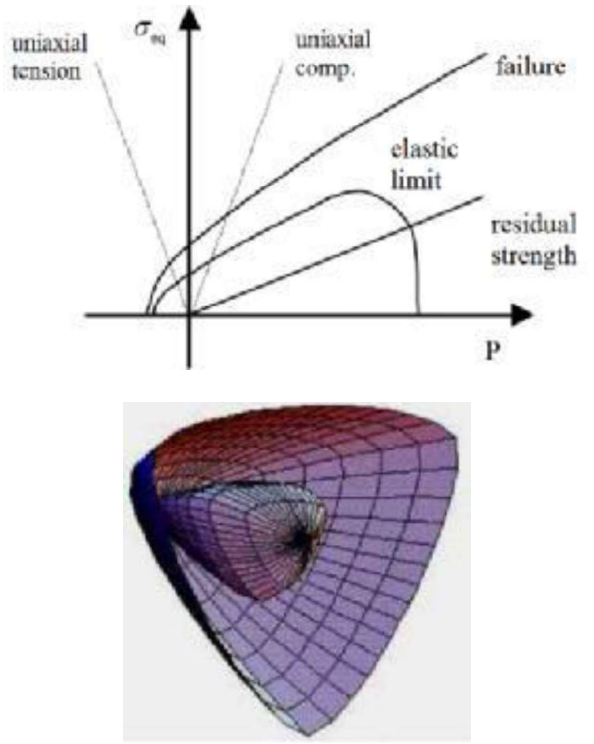

Fig. 2 : Meridian and 3D images of the RHT model [8,9].

The model was ready to estimate the concrete failure; which means that it was able to predict the failure modes of cracking and crushing. Two input strength parameters are quite required to outline a failure surface for the concrete; ultimate uniaxial tensile and compressive strengths. Consequently, the concrete fails because of the multiaxial stress state criterion could be calculated [8,9].

For concrete elements, cracking is completed once the tensile stress in any direction lies outside the failure surface. The modulus of elasticity of the concrete element after cracking becomes zero in the parallel direction to the principal tensile stress. While crushing occurs once all the stress points are found outside the failure surface and are all compressive. Then, the elastic modulus was brought to zero in all directions, and the element disappears effectively [8]. Concrete is assumed to lose its strength and stiffness once the material is crushed.

3.2 Constitutive Relations of Concrete in Compression and Tension

Constitutive modeling of inelastic short-term behavior of concrete has been performed based on different approaches such as non-linear elasticity, elasto-plasticity and fracture models. For the constitutive relations under blast loading, concrete is considered as a quasi-brittle material and of different behavior in tension and compression. The tensile strength of concrete is about 10% of compressive strength. Figure (3) shows a typical stress-strain curve for concrete. In Compression, the stress-strain curve is linear up to 30% of the maximum strength [8] and then the curve follows the following equations:

$$f = \frac{E_c.\varepsilon}{1+\left(\frac{\varepsilon}{\varepsilon_o}\right)^2} \quad (1)$$

$$\varepsilon_O = \frac{2f'_c}{E_c} \quad (2)$$

$$E_C = \frac{f}{\varepsilon} \quad (3)$$

where f = stress at any strain ε, and ε_o = strain at the ultimate compressive strength fc '

On the other hand, in tension, the concrete stress-strain curve is almost linear elastic up to the maximum tensile strength. After this point, the concrete cracks and the strength decreases gradually to zero. The derived equations for this curve are shown below.

$$\sigma_{cu} = k_1.k_2.f_{cu} \quad (4)$$

$$\varepsilon_{co} = k_3.\varepsilon_o \quad (5)$$

$$\sigma_{tu} = k_4.f_{tu} \quad (6)$$

where: f_{cu} Static compressive strength.
f_{tu} Static tensile strength.
ε_{co} Strain at peak stress for confined concrete
ε_o Strain at peak stress for unconfined concrete = 0.002
k_1 Strength increase factor due to confinement
k_2 Dynamic increase factor in compression
k_3 Strain increase factor due to confinement
k_4 Dynamic increase factor in tension

k_1 and k_3 are factors derived as function of yield stress of stirrups and volumetric ratio of stirrups [8]. While the k_2 and k_4 factors are functions of the strain rate of concrete [8].

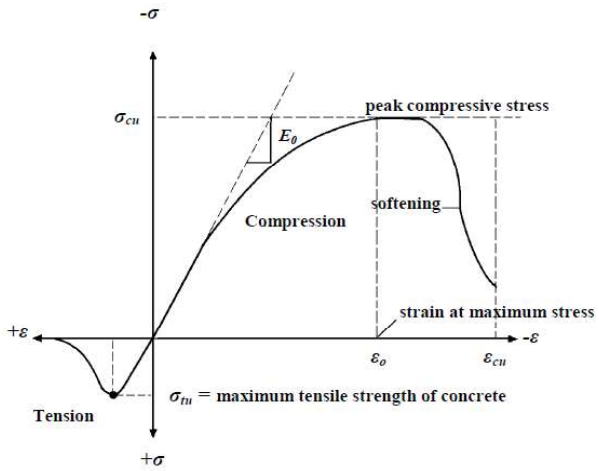

Fig. 3 : Typical Uniaxial Compressive and Tensile Stress-Strain Curve for Concrete[8,9].

4. Material Modelling of Steel reinforcement

In 3-D stress space, Johnson–Cook constitutive model is used for finite element simulation [8,9] that due to its ability to simulate materials behavior subjected to massive strains, high strain rates and high temperatures. These factors are obtained from intense impulsive loading caused from high velocity impact and/or explosive detonation. For steel, erosion models are accustomed management for the failure behavior of such material. The failure model for steel may be a plastic strain value of 0.2%. The steel material fails by reaching such strain. However, the erosion model may be a geometric strain value of 0.2%, and cells are eroded once reached this value. In alternative words, any cell reaches erosion value of 0.2; it is omitted from the calculation. This assists in preventing tiny time steps inflicting termination of the program.

Bilinear elastoplastic stress - strain curve with strain hardening as shown in Figure (4) is used for steel in Compression & Tension [8,9]. Before yielding, the steel stress – Strain constitutive relation is linear and calculated as follows:

$$f_s = E_s \cdot \varepsilon_s \qquad (f_s < f_{yd}) \qquad (7)$$

$$f_s = f_{yd} \qquad (\text{if } \varepsilon_s = \varepsilon_{yd}) \qquad (8)$$

where f_s and ε_s are steel stress and steel strain, respectively.

E_s the elasticity modulus for steel

At yielding point, the steel stress is calculated as follows:

$$f_{yd} = k_s \cdot f_{ys} \qquad (9)$$

where k_s Dynamic increase factor for steel and f_{ys} Static yield stress

After yielding point, the steel stress is calculated taking into account the effect of strain hardening as follows:

$$f_s = f_{yd} + \mathrm{Eh} \cdot (\varepsilon_s - \varepsilon_y) \qquad (10)$$

where E_h is the hardening modulus for steel and is taken as 0.1 E_s .

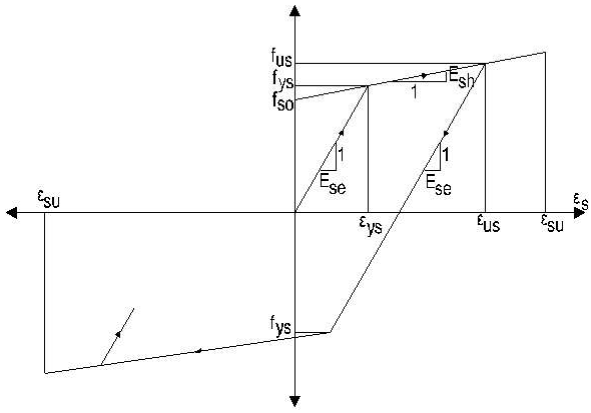

Fig. 4 : Stress-Strain Curve for Steel Reinforcement [8,].

5. Prediction of Dynamic Response of Square RC Columns

5.1. Description of Finite Element Model

The study presents a comparison between the experimental results as measured by Siba [10] with the predictions of AUTODYN program [8,9]. Two Square RC columns, experimentally tested cases (CONV-2) and (CONV-10), were chosen to be numerically modelled and validated. The stand-off distance varied from one test to another [10]. For CONV-2, it was 1.3 m, while for CONV-10 it was 2.66 m. The column specimens were modeled numerically in the FE program, simulating the experimental 123 Kg of TNT explosive, which was placed at a height of 0.65 m above the ground, For blast loading, peak pressure during experimental test was (51 MPa) for CONV-2, and (30.376 MPa) for CONV-10. The predicted overpressure by AUTODYN was (52.3 MPa) for CONV-2, and (29.73 MPa) for CONV-10. The material properties of air, steel, and concrete are all retrieved from the AUTODYN material libraries.

For CONV-2 and CONV-10 tests, the columns [10] as shown in Figure (5) and Table (1) are square concrete specimens with compressive strength of 35 MPa and having dimensions of 300 x 300 mm, with height of 3200 mm. The reinforcement enclosed by the concrete comprises 4 longitudinal bars of diameter equals 19.5 mm with yield strength (Fy) equals 474.4 MPa and yield strain of 0.22%, horizontal stirrups of diameter equals 11.3 mm spaced every 300 mm with yield strength of 465.2 MPa, the concrete cover was 40 mm in all sides.

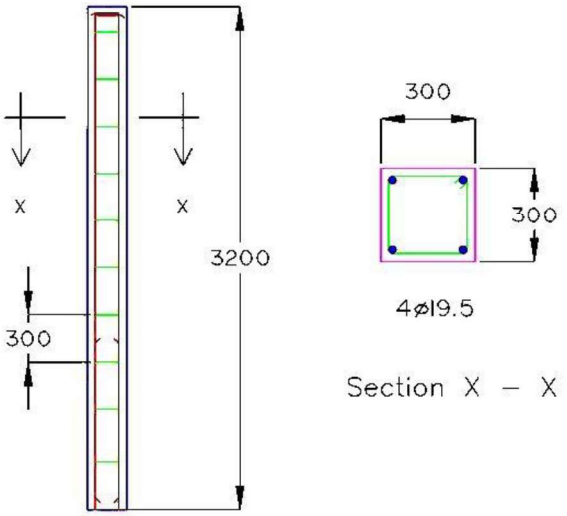

Fig. 5 : Details of Square Column Specimen [10].

Table 1 : Basic data for Square Columns [10]

Model by		Farouk Siba [10]
Concrete Dimensions (mm)		300 x 300
Height (mm)		3200
Concrete Cover (mm)		40
F_{cu} (MPa)		35
Longitudinal RFT	Bar Diameter (mm)	**4 □ 19.5**
	F_y (MPa)	474.4
Transverse RFT	Stirrups Diameter (mm)	11.3
	Stirrups Spacing (mm)	300
	F_y (MPa)	465.2
Charge weight (kg)		123 Kg of TNT
CONV-2 Stand-off Distance (SOD) mm		1300
CONV-2 Pressure (MPa)		51 MPa
CONV-10 Stand-off Distance (SOD) mm		2660
CONV-10 Pressure (MPa)		30.376 MPa

In both of the AUTODYN simulations presented, the finite element mesh of the Euler-FCT Air space contains 384000 cells with a grid of 80×30×160 nodes graded zoning. The cell dimension is chosen in such a way that one Euler-FCT cell cover half of the smallest concrete cover of a column specimen (40 mm) to simulate the striking media. The RC column specimen is represented by 18000 Lagrange cells with a grid of 8×8×80 cells. Steel bars are represented by 78 beam cells with a grid of 1×78 cells.

5.2. Predicted Behavior and Failure Modes

Figure (6) compares the predicted and observed failure modes where a good agreement is achieved. For column CONV-2, extensive cracking & spalling of concrete revealing reinforcement in the lower one-third region of the column were predicted because of the location of the blast near the ground. Buckling of the bar in the back face of the column was observed. Minimal flexural cracks were also observed on the column. These cracks were wider on the back face and sides of the column. The spalling & cracking of concrete in the lower part of the column, close to the concrete footings, are seen in Figure (6).

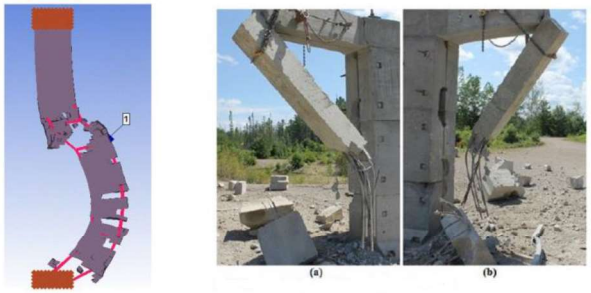

Fig. 6 : Predicted and Observed Failure Pattern for Square Column CONV-2 [8].

From the comparison of the numerical and experimental results in Figure (7), a good agreement is noticed. For Column CONV-10, substantial cracking and spalling of concrete cover revealing longitudinal reinforcement in the lower one-third region of the column were predicted. Minimal flexural cracks were observed on the back-face column. Within the lower one-third region, substantial shear cracks were observed as shown in Figure (7).

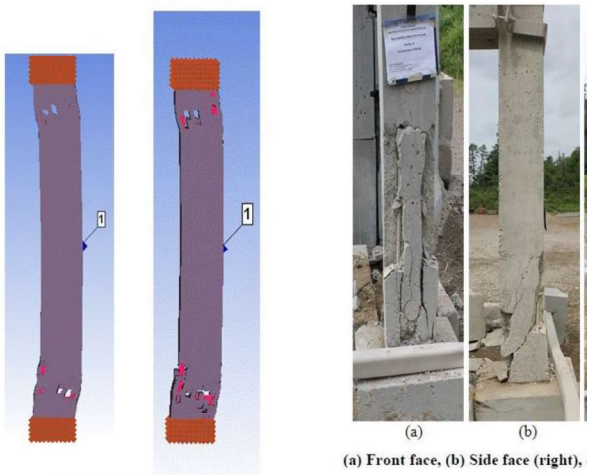

Fig. 7 : Predicted and Observed Failure Pattern for Square Column CONV-10 [8].

5.3. Predicted Displacement and Acceleration Histories

Figures (8) & (9) demonstrate the comparison of displacement history curves between both the experimental and AUTODYN results. All the resulted curves display the time on the horizontal axis given in (msec), and the displacement on the vertical axis given in (mm). It is noticed that the AUTODYN results are close to the experimental proposed results; both the experimental and the finite element analysis are in good agreement with each other's. Also, it was found that, the peak displacement reached by the experimental study for the tests CONV 2 and CONV 10, was 11.05 mm and 9.87 mm respectively while the

peak displacement reached by the simulated AUTODYN was 14.28 mm and 11.70 mm respectively. The difference percentage between them can be calculated as 15 % and 11 % respectively.

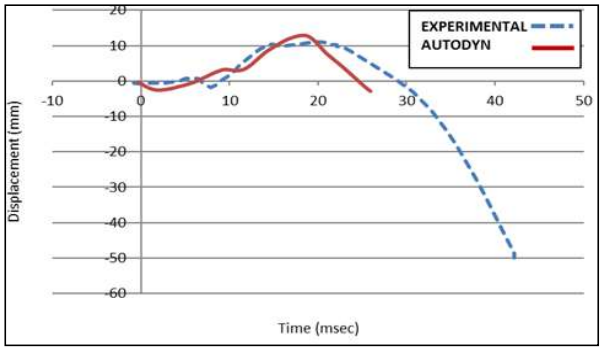

Fig. 8 : Displacement-Time History for Square Column CONV-2 [8].

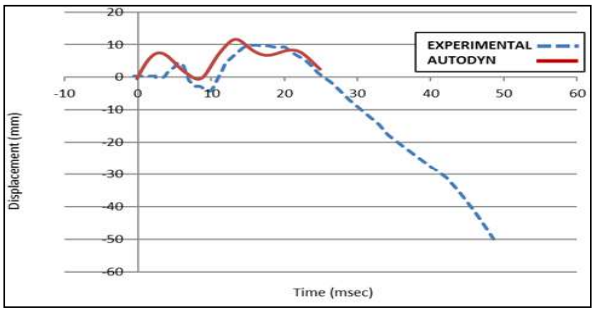

Fig. 9 : Displacement-Time History for Square Column CONV-10 [8].

The predicted acceleration-time curves are shown in Figures (10) & (11), respectively for CONV-2 & CONV-10 tests. The experimental curves were not measured. The peak acceleration reached by the simulated AUTODYN model was 1200 mm/msec^2 and 1523.91 mm/msec^2 respectively.

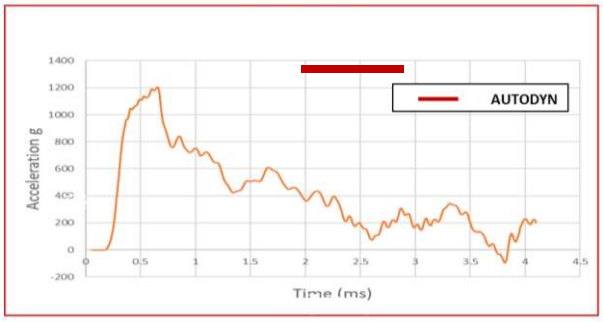

Fig. 10 : Predicted Acceleration-Time History for Square Column CONV-2 [8].

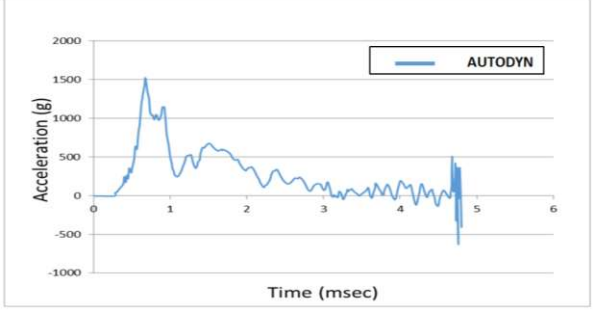

Fig. 11 : Predicted Acceleration-Time History for Square Column CONV-10 [8].

6. Prediction of Dynamic Response of Rectangular RC Columns

6.1. Description of Finite Element Model

The column constructed and tested by Lloyd [11] as given in Figure (12) and Table (2), was a rectangular concrete column model with compressive strength of 58 MPa, of dimensions 100 mm x 150 mm, total height including the two supports of 2438 mm while the free height between the two supports of 1980 mm, the longitudinal reinforcement was 4 bars M10 (one bar at each corner with equivalent diameter of 11.3 mm) with longitudinal reinforcing ratio of 2.67%, with yield strength of 483 MPa, while the horizontal reinforcement (stirrups) are of diameter equals 6.3 mm spaced at 75 mm with volumetric ratio of 1.52% with yield strength of 580 MPa, the concrete covering the longitudinal bars was 20 mm in all sides) [11] . AUTODYN has more than 15 standard material libraries. The material properties of air, steel, and concrete are all retrieved from the AUTODYN material libraries [9].

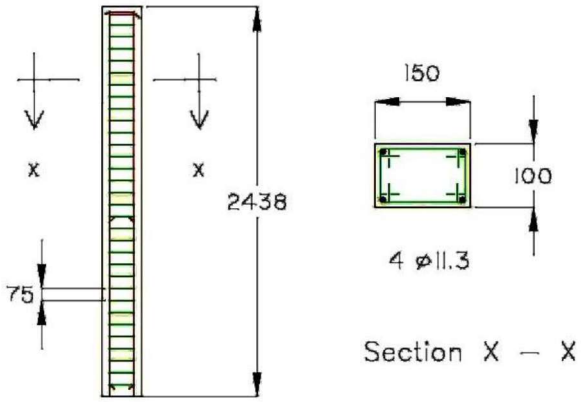

Fig. 12 : Details of Rectangular Column Specimen [11].

Table 2 : Basic data for Rectangular Columns [11]

Model by		Alan Lloyd [11]
Concrete Dimensions (mm)		100 x 150
Height (mm)		2438
Free Height (mm)		1980
Concrete Cover (mm)		40
F_{cu} (MPa)		58
Longitudinal RFT	Bar Diameter (mm)	**4 □ 11.3**
	F_y (MPa)	483
Transverse RFT	Stirrups Diameter (mm)	6.3
	Stirrups Spacing (mm)	25
	F_y (MPa)	580
Equivalent Charge weight (kg)		33.4 Kg of TNT
Equivalent Stand-off Distance (SOD)		1300 mm
Pressure (MPa)		12.02 MPa (Shock Tube)

A numerical model was built in AUTODYN reproducing the experimental test. Given that in the experimental test the concrete blocks did not suffer any

displacement or rotation, the blocks were partially modelled and a velocity value of zero was imposed at the ends of the blocks as boundary condition clamping the member. The symmetry of the problem also allowed modelling a half of the RC member. In the AUTODYN simulations, the finite element mesh of the Euler-FCT Air space contains 1024800 cells with a grid of 140×30×244 nodes graded zoning. The cell dimension is chosen in such a way that one Euler-FCT cell cover half of the smallest concrete cover of a column specimen (20 mm) to simulate the striking media. The reinforced concrete column specimens are represented by 36600 Lagrange cells with a grid of 10×15×244. Steel bars are represented by 242 beam cells with a grid of 1×242 cells.

6.2. Predicted Behavior and Failure Modes

Figure (13) compares the predicted and observed failure modes where a good agreement is achieved. The failure mode expected for the columns as shown in the figure is extensive, due to the absence of retrofitting material, normal column strain and also normal absorbing for the blast wave energy. By using the finite element model, the total maximum mid-height strain for tension steel in column RC-14 was 0.094 %. These strains occurred at 19.8 msec for the mid-height and support locations, respectively, after the start of the shock wave loading. The mid-height tension steel had a 0.013 % residual strain after test 2 for a cumulative residual strain of 0.023%. The tension steel near the support had a residual strain of 0.002. There was also some minor cracking visible in the tension concrete at mid-height of the column [11].

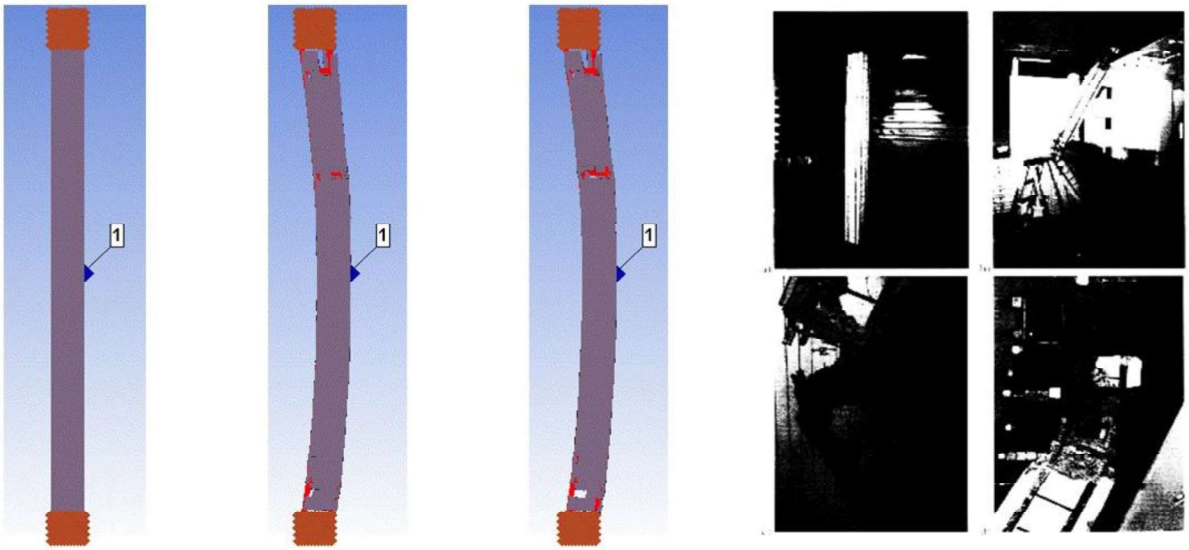

Fig. 13 : Predicted and Observed Failure Pattern for Rectangular Column [8].

6.3. Predicted Displacement and Acceleration Histories

Figure (14) demonstrates the comparison displacement histories curves between both the experimental and AUTODYN results. All the resulted curves display the time on the horizontal axis given in (msec), and the displacement or acceleration on the vertical axis given in (mm) or (mm/msec^2) respectively. It was noticed after running the software program models, that the AUTODYN predictions are close to the experimental proposed results; both the experimental and the finite element analysis are in good agreement with each other's. For the model tested by Alan Lloyd [9] and then validated in our study, it was found that, the peak displacement reached by the experimental study for the RC 3-1 was 15.255 mm, while the peak displacement reached by the simulated AUTODYN was 17.34 mm. The percentage difference between is calculated 10 %.

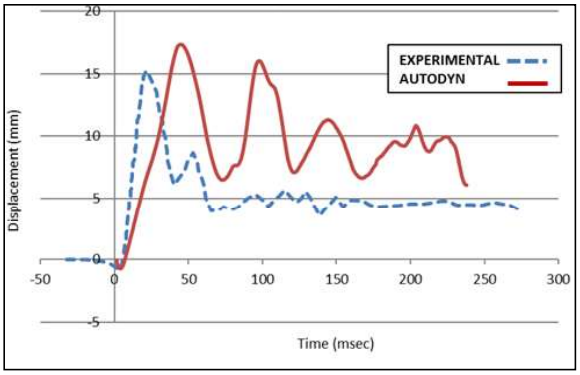

Fig. 14 : Mid-Height Displacement-Time History for Test for Rectangular Column [8].

The predicted acceleration-time curve is shown in Figure (15) for the studied column. The experimental curve was not measured. The peak acceleration reached by the simulated AUTODYN model was 1540 mm/msec^2.

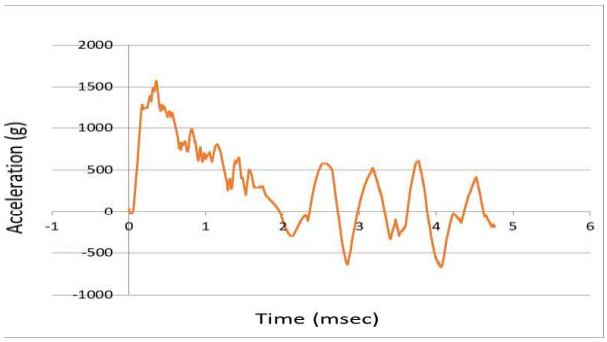

Fig. 15 : Predicted Mid-Height Acceleration-Time History for Rectangular Column [8].

7. Conclusions

The following points are concluded from the modelling and validation studies:

1- The successful validation studies show that the computer code AUTODYN in conjunction with the proposed material models is a good tool for predicting the dynamic behavior of blast-loaded RC columns. Also, the explicit time integration scheme proves to be sufficient for predicting the dynamic response under blast.

2- For concrete in compression, the use of RHT multi-axial model which includes the effects of strain hardening and softening is suitable for simulating the nonlinear compression behavior of concrete. Inclusion of stirrups-induced confinement and strain rate sensitivity effects leads to realistic dynamic analysis.

3- Tensile cracking plays a dominant role in the nonlinear dynamic behavior. The structural response is found to be sensitive to the parameters of crack initiation and crack propagation processes, Also, the inclusion of strain rate dependence in tension is important for nonlinear analysis.

References

[1] Unified Facilities Criteria UFC 3-340-02, "Structures to Resist the Effects of Accidental Explosions ", U.S. Army Corps of Engineers, 2008.

[2] Luccioni, B.M, Ambrosini, R. D. & Danesi, R.F. " Failure of a reinforced concrete

[3] building under blast loads", WIT Transactions, Vol 49, 2015.

[4] Parisi, F., “Blast fragility and performance-based pressure–impulse diagrams of European reinforced concrete columns”, Engineering Structures, ELSEVIER Journal, Vol 103, pp 285 - 297, 2015.

[5] Codina, R., Ambrosini, D., & Borbón, F., " Experimental and numerical study of a RC member under a close-in blast Loading", Engineering Structures, ELSEVIER Journal, Vol. 127, pp 145 - 158, 2016.

[6] Beshara, F.B.A. "Nonlinear Finite Element Analysis of Reinforced Concrete Structures Subjected to Blast Loading ", PhD Thesis, City University, London, 1991.

[7] Beshara, F.B.A., “Smeared Crack Analysis for Reinforced Concrete Structures Under

[8] Blast-Type Loading“, Engineering Fracture Mechanics J., Vol.45, pp.119-140, 1993.

[9] Kadhom, B., " Blast Performance of Reinforced Concrete Columns Protected by FRP Laminates", PhD Thesis, University of Ottawa, Canada, 2016.

[10] Ameen, M.K. “Dynamic Analysis of Retrofitted RC Columns under Blast Loadings”, Banha University, Shoubra Faculty of Engineering, Dep. of Civil Engineering, PhD. Thesis to be submitted, Cairo 2019.

[11] Century Dynamics, AUTODYN User and Theory Manual, 2016.

[12] Siba, F., "Near-Field Explosion Effects on Reinforced concrete Columns: An Experimental Investigation", M.Sc. Thesis, Carleton University, Canada, 2014.

[13] Lloyd, A., " Performance of Reinforced Concrete Columns under Shock Tube

[14] Induced Shock Wave Loading ", PhD Thesis, University of Ottawa, Canada, 2010.